Key Engineering Materials
ISSN: 1662-9795, Vol. 926, pp 280-287
doi:10.4028/p-u9ydck

Submitted: 2021-12-07
Accepted: 2022-02-22
Online: 2022-07-22

Laser-Powder Bed Fusion of Inconel 718 Alloy: Effect of the Contour Strategy on Surface Quality and Sub-Surface Density

Andrea El Hassanin[1,a*], Francesco Napolitano[1,b], Carmela Trimarco[1,c], Emanuele Manco[1,d], Fabio Scherillo[1,e], Domenico Borrelli[2,f], Antonio Caraviello[2,g], Antonino Squillace[1,h] and Antonello Astarita[1,i]

[1]Dept. of Chemical, Materials and Production Engineering, University of Naples "Federico II", Piazzale Vincenzo Tecchio 80, 80125, Naples, Italy

[2]Sòphia High Tech, Via Romani 228, 80048, Naples, Italy

[a*]andrea.elhassanin@unina.it, [b]francesco.napolitano4@unina.it, [c]car.trimarco@studenti.unina.it, [d]emanuele.manco@unina.it, [e]fabio.scherillo@unina.it, [f]domenico.borrelli@sophiahightech.com, [g]antonio.caraviello@sophiahightech.com, [h]squillac@unina.it, [i]antonello.astarita@unina.it

Keywords: Laser-Powder Bed Fusion, Inconel 718, surface roughness, density.

Abstract. The in-situ contour strategy during Laser-Powder Bed Fusion (L-PBF) process remains one of the most promising solutions to improve the poor surface quality of the parts. On the other hand, it is well established that contour step affects the formation of sub-surface defects. The aim of this work is to assess the entity of sub-surface defects during the Laser-Powder Bed Fusion of Inconel 718 samples for which different contour processing conditions are considered. Cubic samples with 10 mm side were produced through L-PBF using a Concept Laser Cusing M2 L-PBF machine. The samples were printed with fixed bulk laser parameters, adopting a layer thickness of 30 μm and a chessboard laser scanning strategy. The in-situ contour conditions were changed in terms of laser scanning speed and hatch zone border. Afterwards, the samples were analyzed in terms of surface roughness (Sa) and sub-surface density through confocal microscopy. The results revealed that the surface roughness was the most affected output as a function of the varied process parameters, including the sample position on the building platform, with values ranging from 13 to 32 μm. On the other hand, the sub-surface density was always higher than 99%.

Introduction

It is well established nowadays that Additive Manufacturing (AM) technologies — a family of processing techniques able to produce near-net shape parts using polymers, metals, ceramics and composites — revolutionized the manufacturing paradigms and pushed forward the industry towards the model of Industry 4.0 [1]. In this context, Laser-Powder Bed Fusion (L-PBF) is one of the leading metal AM technologies that allows the production of complex parts with high quality starting from metal powders, along with Electron Beam-Powder Bed Fusion (E-PBF) and Laser Engineered Net Shaping (LENS®) [2]. Over the last two decades, this technology has been extensively investigated and applied as an effective manufacturing process for several applications, for which a large number of metals and alloys are respectively used [3]. Among these, Inconel 718® (IN718), a nickel-based superalloy, represents one of the most investigated [4]. Since this alloy presents very unique mechanical and physical properties due to a large number of alloying elements, it is employed in critical applications such as hot parts of aircraft engines [4]. In this context, taking advantage of the design flexibility provided by L-PBF overcomes many of the manufacturing limitations of those parts with traditional technologies. Some of these issues concern the machining stability [5], constraints of tools access in specific complex features and the need for extensive assembly operations, despite the fact that L-PBF machines also require this step given the narrow building volumes [6].

On the other hand, in the context of the processing issues when employing L-PBF, both in general and in the specific case of IN718, surface quality remains one of the most challenging especially when considering complex geometry parts. As well known, two fundamental phenomena are detrimental for the surface quality of L-PBF parts (but more generally, for parts made by powder-

based AM technologies): the stair-step effect and the balling effect [7,8]. The first one is strongly dependent from the intended geometry of the desired part, but in general consists in the approximation of a curved surface with a discretized one, due to layer-by-layer material deposition. The second one is always strongly present and has the consequence to leave partially molten metal powders on the surface, whose detrimental effect is worsened if down-looking surfaces are considered [9]. For these reasons, a surface finishing step is required to improve the quality of the produced parts. Generally speaking, post-build treatments are often considered to this aim [10–12], but these could be very time and cost-consuming steps, increasing therefore the lead time and the cost of AM parts. One of the first investigated solutions to reduce the roughness of L-PBF parts was to use the L-PBF machine itself through the so-called contour processing during the build [13]. In brief, it involves the use of the same laser employed for the melting and consolidation of the powder feedstock on the surface contours of the parts, with specific process parameters that allow the surface re-melting, as similarly to the ex-situ equivalent process which is very often used [14–17]. More specifically, using a laser with less heat input, the partially molten powders are re-molten and the latter flow into the valleys of the surface, resulting in an overall reduced surface roughness [18]. However, as highlighted by some authors [19,20], the contour step affects both the surface roughness and the density of the processed material below the surface also as a function of the part positioning over the build platform.

In this work, these variables are considered for the case of L-PBF of the IN718 alloy, with the aim to find any correlation between the contour step settings with the side surface roughness and sub-surface defects of the produced parts.

Materials and Methods

L-PBF samples. In this work, IN718 cubic samples with 10 mm side were produced in collaboration with Sòphia High Tech S.r.l, using a Concept Laser Cusing M2 L-PBF machine. Along with the image illustrating the samples, in Fig. 1 is reported an SEM image illustrating the IN718 powders used, whose chemical composition is reported in Table 1. The powders had a size range of 5-42 μm.

Table 1. Chemical composition (wt%) of the IN718 powders.

Element (wt%)	Al	Cr	Fe	Mo	Ni	Nb	Ti	Cu	Others
	0.7	20.5	18.5	2.9	51.6	4.8	0.8	/	Balance

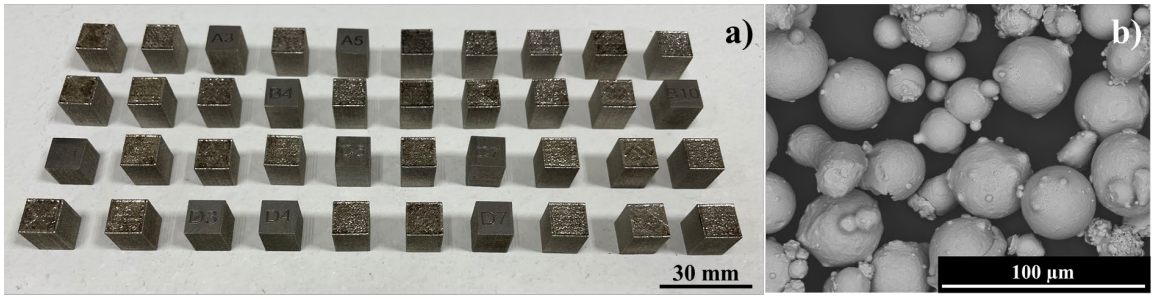

Figure 1. a) L-PBF samples produced and b) SEM image of the IN718 powders used for the L-PBF process (magnification: 1000x).

The L-PBF samples were produced according to the job layout illustrated in Fig.2a, using a chessboard scanning strategy with the aim to reduce the residual stresses [21]. However, with the aim to evaluate the influence of the sample position, laser scan speed and hatch zone border, a sub-set of 12 samples was selected from the full job, as illustrated in Fig.2b. For the sub-set, the investigated process parameters are reported in Table 2.

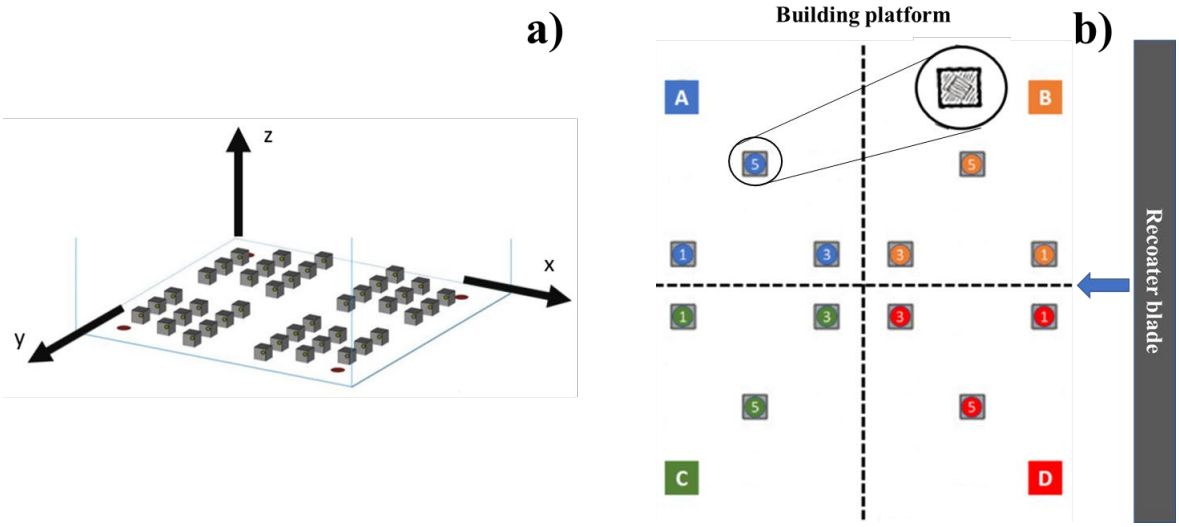

Figure 2. a) L-PBF samples full job b) samples sub-set selected for this work, showing also the island scanning strategy applied to each sample.

Table 2. L-PBF process parameters used for the samples sub-set illustrated in Fig.2b (the IDs refer to all the building platform sectors from A to D).

					bulk		contour		
ID	**Scanning strategy**	**Spot size [mm]**	**Laser power [W]**	**Layer thickness [mm]**	**Speed [mm/s]**	**Hatch spacing**	**Speed [mm/s]**	**Beam compensation [mm]**	**Hatch zone border [mm]**
1	Island	0,15	192	0,03	400	0,15	2000	0,075	0,06
3	Island	0,15	192	0,03	500	0,15	2000	0,075	0,065
5	Island	0,15	192	0,03	800	0,15	1200	0,075	0,065

Characterization procedure. After the L-PBF process, the as-built samples were accurately cleaned in an ethanol ultrasonic bath for 10 min. To evaluate the surface roughness, a Leica DCM3D confocal microscope was used to acquire a single side of each sample, according to the scheme reported in Fig. 3. Each acquisition was carried out considering a 10x magnification and an area of 5 mm x 5 mm centered on the side 1 of the sample. After the acquisition, tilt correction and missing points filling operations were performed on the acquired datapoints through the LeicaMap v7® software. Finally, the areal arithmetic mean of the heights distribution (Sa) was evaluated from each acquisition according to the ISO 25178 standard [22].

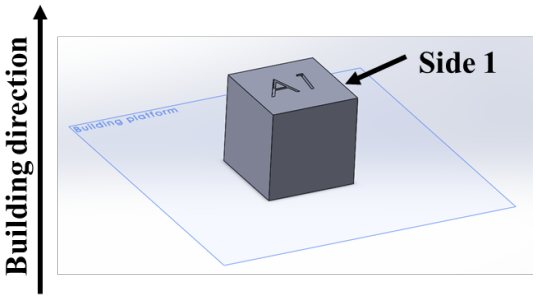

Figure 3. A sample sketch that illustrates the side 1 considered for the surface roughness and sub-surface density evaluation.

After the surface roughness evaluation, the samples were cut in a plane parallel to the scanning strategy at the half height of the build, in order to perform the standard metallographic preparation procedure [23]. Afterwards, confocal microscope acquisitions were carried out again with the aim to

acquire the cross-sectional view of each sample, as illustrated in the example reported in Fig.4a. In this case, the acquisition area covered an entire side of the sample (the same as the one chosen for the roughness evaluation) and a depth of 1.5 mm. The image of each sample was then imported in Matlab® with the aim to measure the area fraction of the sub-surface defects in the region that intersects the bulk and the contour zones. In other terms, according to the scheme reported in Fig. 4b, the region of interest is the overlap region given by the 75 µm deep contour zone (see beam compensation in Table 2) and the hatch zone border that represents the distance from the surface of the island scanning strategy (i.e, bulk) zone. In order to ensure that this region was always considered for the analysis as a function of the variable hatch zone border, a 20 µm wide crop area was considered from each cross-sectional view and then used for the void calculation.

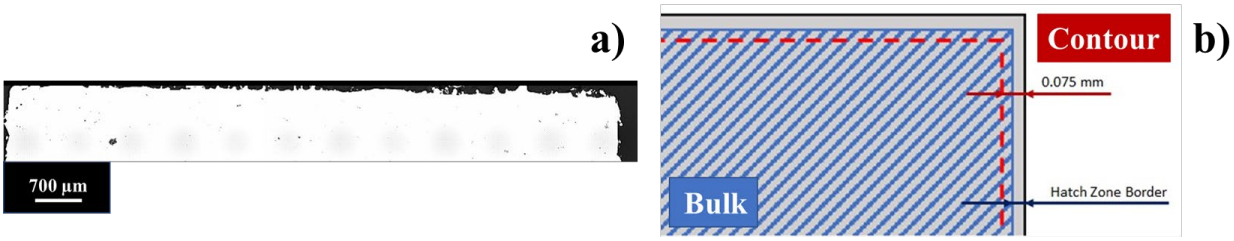

Figure 4. a) Example of a cross-sectional view used for the analysis and b) scheme of the regions involved in the analysis (the cropped region is the intersection between the red and blue areas, taken from one side of each sample).

Results and Discussion

In Fig. 5 are showed the roughness values measured for the investigated samples, sorted by the ID number and compared between the four sectors representing the build platform. As a general consideration, it can be noted that the different conditions led to significantly different roughness values, ranging globally from 11 to 32 µm. However, more specific considerations can be highlighted: i) the samples #5, regardless of the sector, had always the lowest roughness values; ii) the samples #1 represent always the worst surface quality condition, if not comparable to samples #3; iii) an appreciable difference in trend can be noted by comparing the sectors A-C and B-D. According to the aforementioned points, these experimental outcomes could be explained considering the following issues: i) the samples #5, despite the use of a higher scanning speed for the bulk region, has the lowest roughness due to the employment of a reduced contour scanning speed. This can be explained considering the balling phenomenon, for which an insufficient heat input implies an unstable melting track, determining the formation of separated molten balls that adversely affects the final surface quality [8]; ii) the samples #1 do suffer of the not advantageous position on the build platform: given the edges of the latter, the powder bed spreading process could be quite different in comparison with the inner part [24], determining therefore a different laser-matter interaction even at fixed laser process parameters; iii) the influence of the powder spreading process justifies also this point, considering also that feedstocks with a wide powder size distribution may induce, in the case of the bigger powders, the formation of an agglomerated front as the recoater moves across the platform. This effect, as expected, is more pronounced when considering the platform edges (see samples #1).

Furthermore, another variable that introduce a different contribution on the final surface quality of the parts with fixed laser parameters is the island scan strategy. As highlighted by [19] in their similar work focused on the AlSi10Mg alloy, the scanning strategy (in their work, linear) affects the final surface as a function of the sample position, given that sometimes the side surface is not remelted with an entire contour track, but rather a portion. In this work, similar conclusions could be drawn given that the scanning strategy is applied on the entire build platform, and not to the individual sample.

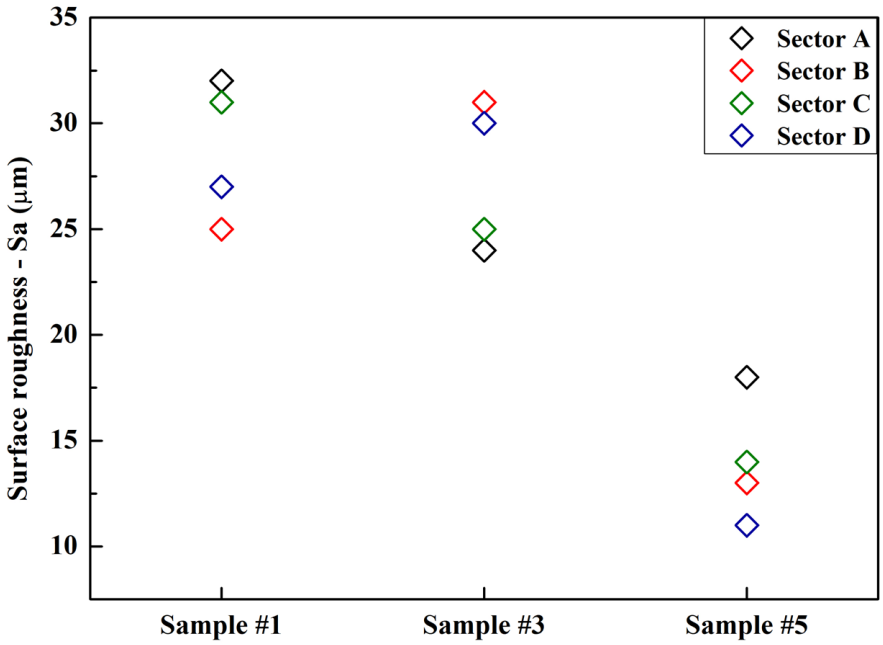

Figure 5. Surface roughness plot of the investigated samples.

The surface quality differences between the samples quantified by means of confocal microscopy can be seen qualitatively also from their cross-sectional view illustrated in Fig. 6. From each the latter, the 20 μm wide crop area was extracted in order to quantify the sub-surface metallographic density through Matlab®. The results of the calculation are synthetically reported in Table 3. From the results, it is easy to observe that the different contour process parameters had no significant effect on the void formation, since every condition led to values above the 99%. This experimental outcome demonstrates therefore that, within the investigated process window, a correlation between the effects of the contour strategy conditions on both surface quality and sub-surface density cannot be observed.

Table 3. Sub-surface density of the investigated samples.

Sub-surface density (%)	Sector A	Sector B	Sector C	Sector D
Sample #1	**99.94**	**99.94**	**99.06**	**99.33**
Sample #3	**99.994**	**99.09**	**99.70**	**99.39**
Sample #5	**99.82**	**99.63**	**100.00**	**99.94**

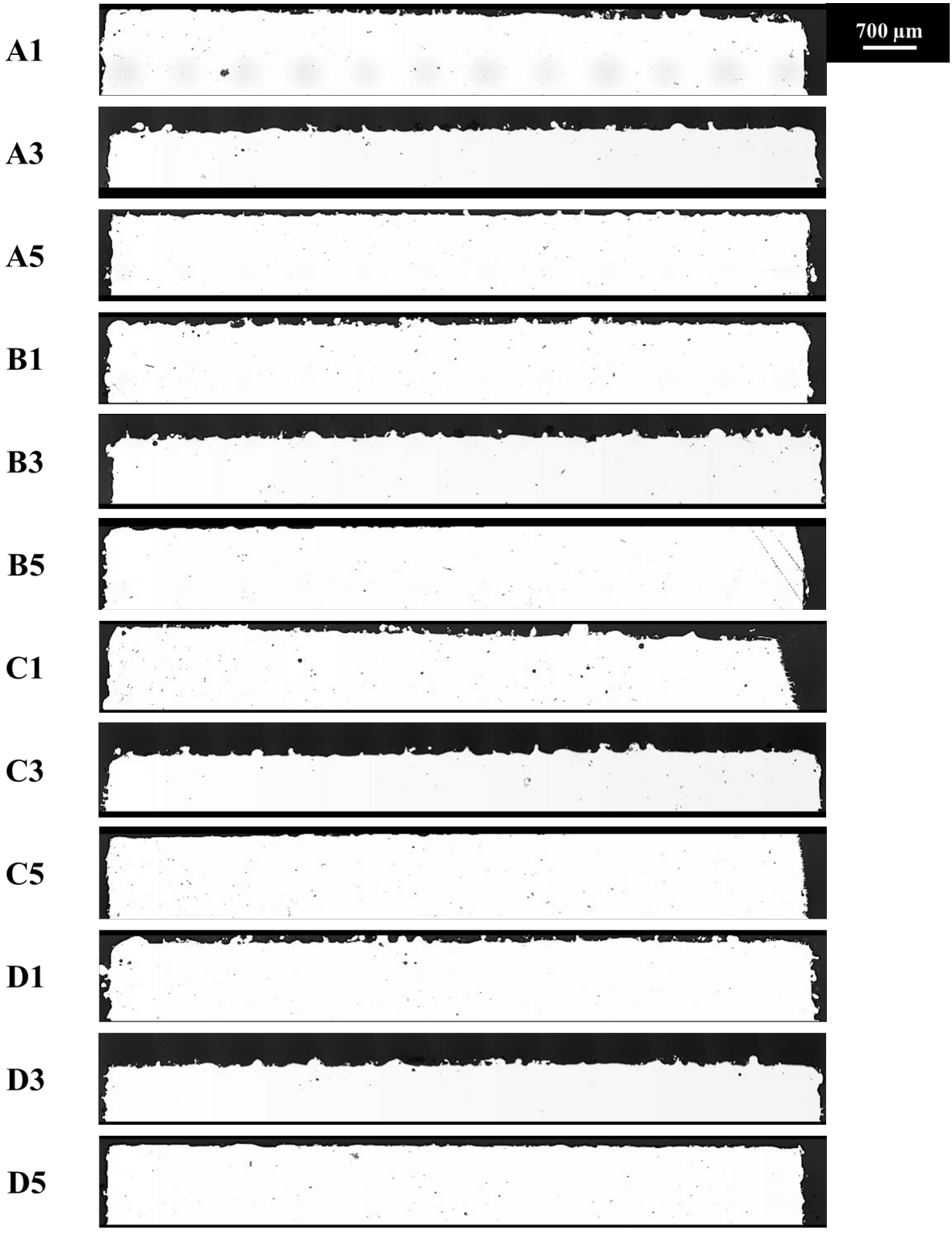

Figure 6. Cross-sectional view of the investigated samples (the upper long side refers to side 1).

Conclusions

This work was focused on the evaluation of the effects of different contour process parameters on the surface roughness and sub-surface density during the L-PBF process of IN718 alloy, giving also attention to the influence of the samples position on the building platform on the measured outputs. On the basis of the obtained results, the following conclusions can be drawn:

- The surface roughness of the printed samples was ranging from 11 to 32 μm, providing a first signal of different effect of the investigated variables;
- The laser scanning speed parameter of the contour step had a more significant effect on the surface roughness: the lowest values of the latter were achieved when the laser speed was set at 1200 mm/s.
- The samples position had a significant effect on the surface roughness as well through the influence of the powder spreading process on the build platform. The worst condition is related to the edges of the platform, for which the loose powders bed layer is not compact as at the middle;
- The island scanning strategy used in this work with the aim to reduce the residual stresses introduce a contribution on the surface quality that is difficult to be quantified, since a different portion of the pattern is applied on each sample;
- The different contour conditions had no significant effect on the sub-surface metallographic density, since the latter was always greater than the 99%.

References

[1] H. Parmar, T. Khan, F. Tucci, R. Uhmer, P.Carlone, Advanced robotics and additive manufacturing of composites: towards a new era in Industry 4.0, Mater. Manuf. Process. 00 (2021) 1–35.

[2] W.E. Frazier, Metal additive manufacturing: A review, J. Mater. Eng. Perform. 23 (2014) 1917–1928.

[3] C.Y. Yap, C.K. Chua, Z.L. Dong, et al, Review of selective laser melting: Materials and applications, Appl. Phys. Rev. 2 (2015).

[4] S. Sanchez, P. Smith, Z. Xu, et al, Powder Bed Fusion of nickel-based superalloys: A review. Int. J. Mach. Tools Manuf. 165 (2021).

[5] B.K. Subhas, R. Bhat, K. Ramachandra, et al, Simultaneous Optimization of Machining Parameters for Dimensional Instability Control in Aero Gas Turbine Components Made of Inconel 718 Alloy, J. Manuf. Sci. Eng. Asme 122 (2000) 586–590.

[6] A. El Hassanin, C. Velotti, F. Scherillo, et al, Study of the solid state joining of additive manufactured components. RTSI 2017 - IEEE 3rd Int. Forum Res. Technol. Soc. Ind. Conf. Proc. (2017);

[7] G. Strano, L. Hao, R.M. Everson, et al, Surface roughness analysis, modelling and prediction in selective laser melting, J. Mater. Process. Technol. 213 (2013) 589–597.

[8] T. DebRoy, H.L. Wei, J.S. Zuback, et al, Additive manufacturing of metallic components – Process, structure and properties, Prog. Mater. Sci. 92 (2018) 112–224.

[9] S. Rott, A. Ladewig, K. Friedberger, et al, Surface roughness in laser powder bed fusion – Interdependency of surface orientation and laser incidence, Addit. Manuf. 36 (2020) 101437.

[10] J.Y. Lee, A.P. Nagalingam, S.H. Yeo, A review on the state-of-the-art of surface finishing processes and related ISO/ASTM standards for metal additive manufactured components, Virtual Phys. Prototyp. (2020);

[11] F. Scherillo, E. Manco,A. El Hassanin, et al, Chemical surface finishing of electron beam melted Ti6Al4V using HF-HNO3 solutions, J. Manuf. Process. 60 (2020) 400–409.

[12] A. El Hassanin, M. Troiano, A.T. Silvestri, et al, Influence of abrasive materials in fluidised bed machining of AlSi10Mg parts made through selective laser melting technology, Key Eng. Mater. 813 (2019) 129–134.

[13] H. Jia, H. Sun, H. Wang, et al, Scanning strategy in selective laser melting (SLM): a review, Int. J. Adv. Manuf. Technol. 113 (2021) 2413–2435.

[14] J. Li, D. Zuo, Laser polishing of additive manufactured Ti6Al4V alloy: a review, Opt. Eng. 60 (2021) 1–16.

[15] A. El Hassanin, M.A. Obeidi, F. Scherillo, et al, CO2 laser polishing of laser-powder bed fusion produced AlSi10Mg parts, Surf. Coatings Technol. 419 (2021) 127291.

[16] A. Sassmannshausen, A. Brenner, J. Finger, Ultrashort pulse laser polishing by continuous surface melting, J. Mater. Process. Technol. 293 (2021) 117058.

[17] Y. Zhao, J. Sun, K. Guo, et al, Investigation on the effect of laser remelting for laser cladding nickel based alloy, J. Laser Appl. 31 (2019) 022512.

[18] R. Poprawe, Tailored Light 2 Laser Application Technology, Springer, Berlin Heidelberg, Aachen, 2011.

[19] E. Masiagutova, F. Cabanettes, A. Sova, et al, Side surface topography generation during laser powder bed fusion of AlSi10Mg, Addit. Manuf. 47 (2021) 102230.

[20] E. Beevers, A.D. Brandão, J. Gumpinger, et al, Fatigue properties and material characteristics of additively manufactured AlSi10Mg – Effect of the contour parameter on the microstructure, density, residual stress, roughness and mechanical properties, Int. J. Fatigue 117 (2018) 148–162.

[21] A. El Hassanin, A.T. Silvestri, F. Napolitano, et al, Laser-powder bed fusion of pre-mixed Inconel718-Cu powders : An experimental study, J. Manuf. Process. 71 (2021) 329–344.

[22] ISO. BSI Standards Publication Geometrical product specifications (GPS) — Surface texture : Areal Part 2 : Terms , definitions and surface. 2012.

[23] K. Geels, D. Fowler, W.U. Kopp, et al, Metallographic and Materialographic Specimen Preparation, Light Microscopy, Image Analysis and Hardness Testing, 2007.

[24] V. Lampitella, M. Trofa, A. Astarita, et al, Discrete Element Method Analysis of the Spreading Mechanism and Its Influence on Powder Bed Characteristics in Additive Manufacturing, Micromachines 12 (2021).